

# Effect of hydrogen bonds on protein stability

Valentino Bianco<sup>1</sup>, Svilen Iskrov<sup>1,2</sup>, Giancarlo Franzese<sup>1</sup>

<sup>1</sup>Departament de Física Fonamental, Universitat de Barcelona

Diagonal 647, 08028 Barcelona, Spain

<sup>2</sup>École Normale Supérieure de Cachan, 61, avenue du Président Wilson 94235 Cachan cedex, France

E-mail: gfranzese@ub.edu

**Abstract.** The mechanism of cold- and pressure-denaturation are matter of debate. Some models propose that when denaturation occurs more hydrogen bonds between the molecules of hydration water are formed. Other models identify the cause in the density fluctuations of surface water, or the destabilization of hydrophobic contacts because of the displacement of water molecules inside the protein, as proposed for high pressures. However, it is clear that water plays a fundamental role in the process. Here, we review some models that have been proposed to give insight into this problem. Next we describe a coarse-grained model of a water monolayer that successfully reproduces the complex thermodynamics of water and compares well with experiments on proteins at low hydration level. We introduce its extension for a homopolymer in contact with the water monolayer and study it by Monte Carlo simulations. Our goal is to perform a step in the direction of understanding how the interplay of cooperativity of water and interfacial hydrogen bonds affects the protein stability and the unfolding.

*Keywords:* Water. Hydrated proteins. Confined Water. Biological interfaces. Protein denaturation.

## 1. Introduction

One of the most intriguing challenge in biological physics is the nature of protein folding-unfolding processes. The temperature range of stability of proteins is in general small. For example, staphylococcal nuclease (Snase—a small protein containing 149 amino-acids) folds at low pressure is approximately between 260 K and 320 K [1].

Heat destabilizes proteins. By increasing the bath temperature  $T$ , thermal fluctuations increase and disrupt the folded configurations of proteins. Usually, by decreasing  $T$ , proteins crystallize, but surprisingly some proteins unfold at sufficient low temperature instead of crystallizing [1, 2, 3, 4, 5, 6, 7]. Cold denaturation seems to be a general phenomenon for proteins, generally occurring well below 0°C, the freezing point of water. In some cases, for example for Snase [1], the cold denaturation cannot be directly observed, but experimental data can be extrapolated to predicted the lower temperature of stability for the protein. More generally, to make the cold denaturation observable destabilizing agents can be used. Interestingly, Pastore et al. [2] observed that Yeast frataxin under physiological conditions undergoes cold denaturation below 7°C and remains folded up to 30°C. Hence, Yeast frataxin could be an excellent prototype for studying folding-unfolding transition, both hot and cold, under accessible conditions.

Proteins can unfold also by pressurization. It has been observed that the increase of pressure induces the unfolding of protein [8, 9]. The pressure-unfolding process can be rationalized by considering that the folded structure usually includes cavities. High pressure can induce elastic response of the protein, deforming its structure and pushing water molecules inside the cavities. The water molecules from inside would swell the protein, with consequent loss of protein functionality [8]. Because is difficult to separate the protein response to high hydrostatic pressure from the response of the aqueous environment, the understanding of the problem is still under debate.

### 1.1. Thermodynamics of proteins unfolding

By increasing the thermal energy  $k_B T$  ( $k_B$  is the Boltzmann constant), the protein residues vibrate faster, accessing new possible configurations, i. e. increasing the entropy  $S$  of the system. This increase leads to the hot denaturation, in the same way an increase of  $k_B T$  leads to the melting of a crystal.

The cold denaturation instead, cannot be explained as the effect of an increase of entropy. By decreasing  $T$ , the entropy of the system decreases. This is why we cannot melt a crystal by cooling. Hence, in the case of proteins there must be a complex mechanism that induces the cold denaturation. To understand this mechanism is necessary to introduce the concept of Gibbs free energy  $G \equiv H - TS$ , where  $H \equiv U + PV$  is the enthalpy of the system,  $U$  internal energy of the system,  $V$  the volume and  $P$  the pressure.

General principles of thermodynamics tell us that at any value of  $T$  and  $P$  the system minimizes its Gibbs free energy, where the system, in our case, is the solution of

proteins and water. Hence, the free energy balance must take into account both water molecules and protein residues. The experimental fact that solvated proteins unfolds by decreasing  $T$  means that at lower  $T$  the difference

$$\Delta G \equiv G_u - G_f \quad (1)$$

between the unfolded ( $u$ ) and folded ( $f$ ) states is

$$\Delta G = \Delta H - T\Delta S < 0, \quad (2)$$

where  $\Delta H \equiv H_u - H_f$  and  $\Delta S \equiv S_u - S_f$ .

The total variation of the entropy of the system is given by  $\Delta S = \Delta S_p + \Delta S_w$  where  $\Delta S_p$  and  $\Delta S_w$  are the variation of entropy of the protein residues and water molecules, respectively. By unfolding, the protein entropy increases,  $\Delta S_p > 0$ . On the other hand, the protein contribution to  $\Delta H$  is positive,  $\Delta H_p > 0$ , because the enthalpy of the protein increases when the protein unfolds ( $H_p$  is proportional to the number of contact points of the protein). Therefore, the protein contribution to  $\Delta G$ ,  $\Delta H_p - T\Delta S_p$ , could be negative or positive depending on the relative variations and on  $T$  and does not guarantees that Eq. (2) is satisfied. Hence, water contribution to the total balance of Eq. (2) could be relevant. To date, is widely shared the idea that the native-folded state is stabilized by the quasi-ordered network of water molecules hydrating the non-polar monomers [?].

### 1.2. Protein Phase Diagram

Experiments are consistent with a protein stability phase diagram with an elliptic shape [1, 2, 3, 4, 5, 10] in  $P - T$  plane (Fig. 1). Outside the elliptic region the protein unfolds losing its biological function. Following Hawley [11, 12], we can calculate  $\Delta G$  of the whole system (protein and water) assuming that a protein can stay in only two distinct states, folded and unfolded as in Eq. (1).

Because the internal energy of the system  $U$  is a state variable, we can express its infinitesimal variation  $dU$  as a function of two thermodynamical quantities. If we assume that the unfolding process can be described by infinitesimal quasi-static transformations, applying the First Law of Thermodynamics, we get

$$dU = \delta Q - \delta W, \quad (3)$$

where  $\delta Q$  and  $\delta W$  are the infinitesimal heat absorbed and the infinitesimal work done by system, respectively, along the generic transformation. Since at constant  $T$  and  $P$  is  $\delta Q = TdS$  and  $\delta W = PdV$ , we can express the internal energy variation, for a constant number of particles  $N$ , as

$$dU = TdS - PdV \equiv dU(S, V). \quad (4)$$

Differentiating  $H = U + PV$  we get

$$dH = dU + PdV + VdP = TdS + VdP \equiv dH(S, P), \quad (5)$$

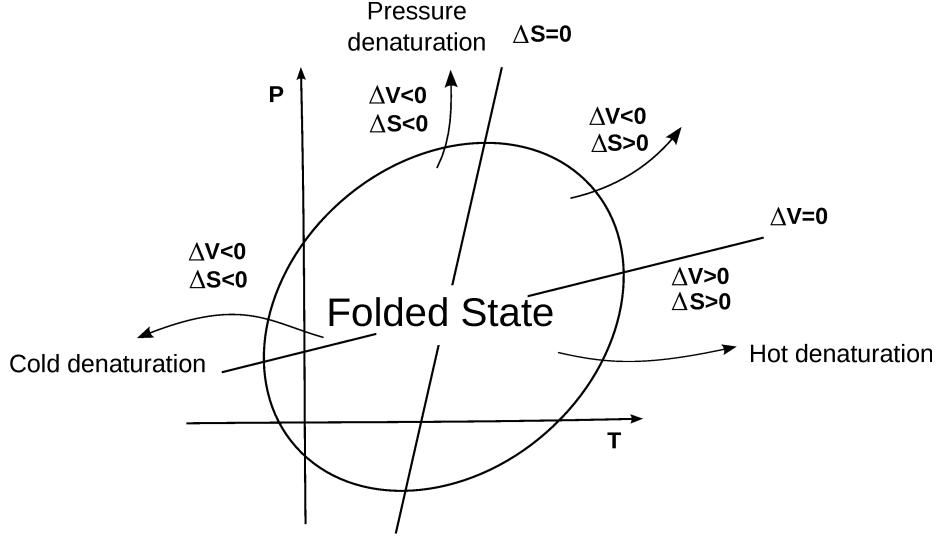


**Figure 1.** Schematic representation of the phase diagram of a protein. Within the elliptic shape the protein is folded, while it unfolds by increasing temperature  $T$  (hot denaturation), by decreasing  $T$  (cold denaturation), by increasing or decreasing pressure  $P$  (pressure denaturation). Each folding–unfolding process is characterized by different variation of entropy  $\Delta S$  and variation of volume  $\Delta V$ . The axes of the ellipse are loci where  $\Delta S = 0$  and  $\Delta V = 0$  (see text for discussion). Adapted from [8].

and differentiating  $G = H - TS$ , we finally get

$$dG = dH - TdS - SdT = -SdT + VdP \equiv dG(T, P). \quad (6)$$

Hence, it is

$$d\Delta G = -\Delta SdT + \Delta VdP \quad (7)$$

with  $\Delta S \equiv S_u - S_f$  and  $\Delta V \equiv V_u - V_f$ . By expanding  $\Delta S$  and  $\Delta P$  to the first order around  $\Delta S_0$  and  $\Delta V_0$ , changes at  $T_0$  and  $P_0$ , we get

$$\Delta S = \Delta S_0 + \left( \frac{\partial \Delta S_0}{\partial T} \right)_P (T - T_0) + \left( \frac{\partial \Delta S_0}{\partial P} \right)_T (P - P_0), \quad (8)$$

$$\Delta V = \Delta V_0 + \left( \frac{\partial \Delta V_0}{\partial T} \right)_P (T - T_0) + \left( \frac{\partial \Delta V_0}{\partial P} \right)_T (P - P_0), \quad (9)$$

and from Eq. (7)–(9), by integration,

$$\Delta G(P, T) = \frac{\Delta \beta}{2} (P - P_0)^2 + 2\Delta \alpha (P - P_0)(T - T_0) + \quad (10)$$

$$-\Delta C_P [(T - T_0) - T_0 \ln(T/T_0)] + \Delta V_0 (P - P_0) - \Delta S_0 (T - T_0) + \Delta G_0,$$

where  $\alpha = (\partial V / \partial T)_P = -(\partial S / \partial P)_T$  is the thermal expansivity factor, related to the isobaric thermal expansion coefficient  $\alpha_P$  by  $\alpha_P = \alpha / V$ ;  $C_P = T(\partial S / \partial T)_P$  is the isobaric heat capacity and  $\beta = (\partial V / \partial P)_T$  is the isothermal compressibility factor related to the isothermal compressibility  $K_T$  by the relation  $K_T = -(\beta / V)$ . All the quantities with

the subscript equal to zero are usually referred to ambient conditions. By developing the logarithm to the second order around  $(T_0, P_0)$

$$\ln\left(\frac{T}{T_0}\right) \sim \frac{T - T_0}{T_0} - \frac{(T - T_0)^2}{2T_0^2}, \quad (11)$$

we get

$$\begin{aligned} \Delta G(P, T) = & \frac{\Delta\beta}{2}(P - P_0)^2 + 2\Delta\alpha(P - P_0)(T - T_0) + \\ & - \frac{\Delta C_P}{2T_0}(T - T_0)^2 + \Delta V_0(P - P_0) - \Delta S_0(T - T_0) + \Delta G_0 \end{aligned} \quad (12)$$

that is the equation of an ellipse given the constraint

$$\Delta\alpha^2 > \Delta C_P \Delta\beta / T_0. \quad (13)$$

This condition is guaranteed by the different sign of  $\Delta C_P$  and  $\Delta\beta$ , as can be observed for some proteins, as reported by Hawley [11].

The Eq. (12) is  $\Delta G(P, T)$  Taylor expansion arrested to the second order, holding for  $\Delta\alpha$ ,  $\Delta\beta$  and  $\Delta C_P$  independent of  $T$  and  $P$ , as generally valid. Adding third order terms in the expansion makes minimal effects on the elliptic shape of the stability region.

At maximum pressure  $P_{\max}$  of stability for the protein,  $d\Delta G/dT = \Delta S = 0$ , while at the maximum temperature  $T_{\max}$  of stability,  $d\Delta G/dP = \Delta V = 0$ . Therefore, based on Hawley's theory it is possible to make general predictions about the changes of  $\Delta V$  and  $\Delta S$  as schematically summarized in Fig. 1. This phenomenological theory has no explicit information about the protein structure, and makes strong assumptions, such as, for example, that the protein only has two states, or that equilibrium thermodynamics holds during the denaturation. The last assumption, in particular, implies that the all process would be reversible. Nevertheless, consistency with Hawley's theory is a good test for models of protein unfolding. In the next section we review some of these models. The review does not pretend to be exhaustive, but it has the aim of mentioning a number of positive results of the theory of protein folding.

## 2. Models for protein unfolding

In 1989 Lau and Dill proposed the HP model for protein folding [13]. By assuming that the exposed surface of hydrophobic residues is energetically unfavorable at low  $T$ , the model reproduces the folding of the protein (hydrophobic collapse). The protein is represented as a self-avoiding chain on a lattice. The chain is composed by two different categories of amino acids: H (non-polar) and P (polar). The presence of the aqueous environment is taken into account in an effective way, by introducing an attractive contact interaction between H monomers. No other interactions are present in the system.

Under these hypothesis, the authors show that the features of the folding process depend on the HH energy interaction, the length of the chain, and the specific sequence of H and P monomers. Moreover, for long chains one folded state dominates.

The model has the virtue to reduce the complexity of the folding process to a manageable level. All the electrostatic and chemical properties of each amino-acid are simplified by allowing only two possible states. The degrees of freedom of the solvent are not explicitly included and the driving force for the folding is the hydrophobic interaction of non polar monomers. Nevertheless, the HP model cannot describe cold denaturation. Therefore, the experimental evidence of cold denatured proteins calls for a reconsideration of the hydrophobic interaction and its dependence on temperature and structure of hydration water [4, 5, 6, 7].

Back in 1948, Frank and Evans [14] discussed the tendency of water to form ordered structures around non polar solutes to minimize the free energy cost of solvation. As a consequence, hydrophobic solutes are “structure makers” for water, facilitating the formation of cages around the solute. The effect of these structures around hydrophobic solutes is to reduce the entropy with respect to the bulk and to compensate, approximately, the enthalpy cost for the creation of a cavity to allocate the solute.

As discussed by Muller in 1990 [15], the compensation of the enthalpy implies that water-water hydrogen bonds (HBs) at the interface with the hydrophobic solute are stronger than those in the bulk. This is consistent with the experimental observation that the excess molar heat capacity for a nonpolar solute at infinite dilution in water is positive. This quantity, defined as the difference of the partial molar heat capacity in solution with the heat capacity of the pure liquid solute, is far larger at 25 °C when the solvent is water than for any other solvent [15, 16].

The statement that HBs are stronger at the hydrophobic interface has led to the misconception that water around a hydrophobic solute has an iceberg-like structure. Computer simulations [17, 18], theoretical analysis [19, 20, 21], and neutron scattering studies [22] are inconsistent with iceberg-like structures. Hence, the restructuring of water around a solute seems not to play a relevant role in the hydrophobic effect. Nevertheless, Muller [15] showed that if hydration HBs are enthalpically stronger but fewer than in bulk, a model with two-states HBs can reproduce the sign reversal of the proton NMR chemical shift with  $T$  and the heat capacity change upon hydration.

On the other hand, a common opinion [23, 24] is that the large free-energy change associated to the hydrophobic effect is due to the small size of the water molecules with respect to the solutes, and that the free-energy change associated to the network reorganization around hydrophobic particles is negligible due to compensation of enthalpy and entropy, although it may account for the large heat capacity change upon hydration. This observation apparently ruled out Muller model, where the enthalpy-entropy compensation upon hydration was not present.

Nevertheless, Lee and Graziano in 1996 [25] showed that Muller model can be slightly modified to recover also the enthalpy-entropy compensation upon hydration. The Muller-Lee-Graziano model was further simplified by De los Rios and Caldarelli in 2000 [26, 27, 28] in order to reduce the number of parameter. By further simplifying the the description of bulk water, they recovered hot and cold denaturation for a protein represented as a hydrophobic homopolymer. A development of this model has been

recently used to study the effective interaction between chaotropic agents and proteins [29].

The model by De los Rios and Caldarelli has been generalized by Bruscolini and Casetti [30, 31] in 2000 by allowing each monomer of non-polar homopolymer to be in contact with a cluster of water molecules. Each cluster has an infinite number of possible states and only one state minimizes the free-energy cost of the interaction with the hydrophobic monomers. The model reproduces the trends of thermodynamics averages in accordance with experiments [32] and simulations [33], and predicts the warm and cold denaturation. These results are qualitatively similar to those of the Muller-Lee-Graziano model, further supporting the relevant role of the solvent in the folding-unfolding process.

Cold denaturation and  $T$ -dependence of the hydrophobic effect were also observed by Dias et al. analyzing a nonpolar homopolymer in Mercedes-Benz (MB) water [34]. The MB model, originally introduced by Ben-Naim [35], represents water molecules as disks in two-dimensions with three possible HBs (arms) as in a Mercedes-Benz logo. Water molecules interact via van der Waals potential and HB interactions. HB interaction is modeled with a Gaussian potential, favoring a fixed value for the water-water distance and aligned arms for facing molecules. Simulations show that the average HB energy is higher for shell water than for bulk water at high  $T$ , while is lower at lower  $T$ . Therefore, by cooling the solution, is energetically more convenient to increase the protein surface exposed to water, inducing protein unfolding. In this model, the water molecules forming a cage around the protein monomers are strongly H-bonded to each other. The highly ordered structure of the solvent around the monomers decreases the entropy of water, compensating the increase of the entropy associated to the protein unfolding.

This model has been criticized [36] because it assumes, without proof, that the enthalpy gain dominates at low  $T$ , giving rise to free-energy gain upon unfolding of the protein. In particular, Yoshidome and Kinoshita [36] analyzed by integral equation theory the behavior of a nonpolar homopolymer composed by fused hard-spheres of different diameters immersed in smaller hard spheres, with permanent electrostatic multiple moments, representing the solvent [37]. The protein-water interaction is represented by a hard sphere potential and water-water interaction by a hard sphere potential and an electrostatic contribution given by the electrostatic multipole expansion. The author found that denaturation is characterized by large entropy loss and large enthalpy gain. However, these two contributions to the free energy almost completely cancel out and make no significant contribution to the free-energy change. They found that the driving mechanism for cold denaturation is the translational entropic-loss of water due to the large excluded volume of the hydrophobic particles. They observed that at low  $T$  water diffuses less, therefore the hydrophobic effect is weaker and the protein unfolds.

### 2.1. Pressure effects

Pressure effects on protein denaturation have been also considered in microscopic theoretical models. For example, in 2003 Marqués and coworkers [38] considered a hydrophobic homopolymer, represented as self-avoiding random walk, embedded in a water bath on a compressible lattice model in two-dimensions. Water–water interactions are represented by the Sastry et al. water model [39]. The polymer–water interaction is repulsive, being proportional to the density number of HBs and to the number of the missed native contact points of the protein. The model displays warm denaturation, pressure denaturation and cold denaturation at high pressure in agreement with stability diagram of some proteins [40], although not with others [41]. A peculiarity of this model is that the effective repulsion between protein and solvent is coupled to the average number of HBs of bulk water.

To remove this coupling to an average property of the bulk, in 2007 Patel and coworkers [42] proposed a model where water at the interface with protein has a restricted number of accessible orientations for the HBs compared to the bulk. Along with the entropic cost, the interfacial HBs also have an additional enthalpic bonus with respect to bulk water, following the ideas discussed by Muller, Lee and Graziano. The model displays a stability phase diagram with hot, cold and pressure denaturation. However, it does not reproduce all the expected features the schematic phase diagram of Fig. (1). In particular, the model does not reproduce the elliptic shape of the phase diagram and the low- $P$  region with  $\Delta S > 0$  and  $\Delta V > 0$  for hot denaturation. These results were confirmed by extending the model to the case with heteropolymers.

In the attempt to reproduce the elliptic phase diagram for protein stability, we propose here a model starting from the assumption that HBs at the interface are stronger compared to HBs in bulk water [43]. We'll proceed as follows: in section 3 we describe the model for nano-confined water, in section 4 we summarize recent results for the model, to clarify its water-like behavior. In the section 5 we propose a protein-water interaction mechanism displaying some preliminary results.

## 3. Hydrophobic nanoconfinement for water

We consider a monolayer of water nano-confined between hydrophobic plates. The interaction between water molecules and the surface is represented by a hard-core repulsion. The confinement is such to inhibit the formation of bulk water structures. For example, bulk water is known to preferentially form four HBs with four nearest neighbor molecules in an approximate tetrahedral structure at low temperature and pressure [44]. Hard confinement inhibits the formation of such bulk structure. For example, Kumar et al. [45] found, by molecular dynamics simulations with TIP5P-water confined between flat hydrophobic plates separated by 0.7 nm, an almost-flat monolayer of water molecules, each with four neighbors in an orientationally-disordered square lattice.



To define a tractable model we coarse-grain this structure of water under similar conditions [46, 47, 48, 49]. We divide the volume between the hydrophobic plates, and accessible to water, into  $N$  cells each containing one water molecule and each with volume  $V/N = r^2 h$ , where  $h$  is the separation between the flat planes,  $r > 2r_0$  is the average distance between water molecules, with  $r_0$  equal to the van der Waals radius of a water molecule. The van der Waals attraction (due to dispersion forces) and the repulsive interactions (due to the Pauli exclusion principle) between water molecules are described by a Lennard-Jones interaction

$$U = - \sum_{ij} \epsilon \left[ \left( \frac{r_0}{r_{ij}} \right)^{12} - \left( \frac{r_0}{r_{ij}} \right)^6 \right], \quad (14)$$

where  $r_{ij}$  is the distance between molecules  $i$  and  $j$  and the sum is performed over all the molecules.

To each cell we associate a variable  $n_i = 0, 1$ . If the number density  $\rho_i$  of the cell  $i$  is  $\rho_i r^2 h \geq 0.5$  then  $n_i = 1$ , otherwise  $n_i = 0$ .

To take into account the decrease of orientational entropy due to the formation of HBs, we introduce for each water molecule  $i$  four bonding indices  $\sigma_{ij}$ , one for each possible HB. Each variable  $\sigma_{ij}$  can assume  $q$  different values,  $\sigma_{ij} = 1 \dots q$ . We choose the parameter  $q$  by selecting  $30^\circ$  as the maximum deviation from linear bond (i.e.  $q = 180^\circ/30^\circ = 6$ ). Hence, every molecule has  $q^4 = 1296$  possible orientations.

The covalent (directional) HB attraction component is expressed by the Hamiltonian term

$$\mathcal{H}_{\text{HB}} = -J \sum_{\langle ij \rangle} n_i n_j \delta_{\sigma_{ij}} \delta_{\sigma_{ji}}, \quad (15)$$

where  $J > 0$  represent the covalent energy gained per HB, the sum is over nearest neighbors cells, and  $\delta_{ab} = 1$  if  $a = b$ , 0 otherwise.

The experiments show that the formation of a HB leads to an open structure that induces an increase of volume per molecule [44, 50]. This effect is incorporated in the model by considering that the total volume of the system is

$$V \equiv V_0 + N_{\text{HB}} v_{\text{HB}}, \quad (16)$$

where  $V_0$  is the volume of the system without HBs, and  $v_{\text{HB}}$  is the increment due to the HB.

The term  $\mathcal{H}_{\text{HB}}$  quantifies the two-body component for HB interaction. On the other hand, the distribution of O-O-O angle shows a strong  $T$ -dependence [51] that suggest the presence of many-body component for HB interaction. We quantify this component by the Hamiltonian term

$$\mathcal{H}_{\text{Coop}} = -J_\sigma \sum_i \sum_{(k,l)_i} \delta_{\sigma_{ik} \sigma_{il}}, \quad (17)$$

where  $J_\sigma > 0$  is the characteristic energy of the cooperative component. The sum is performed over the six different pairs  $(k, l)_i$  of arms of the molecule  $i$ . Therefore the total Enthalpy for the water is

$$H = U + \mathcal{H}_{\text{HB}} + \mathcal{H}_{\text{Coop}} + PV = U - (J - P v_{\text{HB}}) N_{\text{HB}} - J N_\sigma, \quad (18)$$

where

$$N_{\text{HB}} \equiv \sum_{\langle ij \rangle} n_i n_j \delta_{\sigma_{ij}} \delta_{\sigma_{ji}} \quad (19)$$

is the total number of HB and

$$N_{\sigma} = \sum_i \sum_{(k,l)_i} \delta_{\sigma_{ik} \sigma_{il}} \quad (20)$$

is the total number of HBs optimizing the cooperative interaction.

#### 4. Results for water model

We study our model by Monte Carlo (MC) simulations and mean-field calculations. MC simulations are performed in the  $NPT$  ensemble where the volume of the system is a stochastic variable. We consider periodic boundary conditions in the directions parallel to the confining surfaces.

##### 4.1. Liquid-gas phase transition and anomalies.

Previous calculations have shown that the system displays a liquid-gas first-order phase transition ending in a critical point  $C$  at approximately  $k_B T_C / \epsilon = 1.9 \pm 0.1$  and  $P_C v_0 / \epsilon = 0.80 \pm 0.05$  [46, 47, 48, 52, 53, 54], in qualitative agreement with mean field results [48, 49, 54].

The model reproduces several anomalies of water. For example, the system presents density anomaly, i.e. the isobaric increase of density upon cooling, up to reach a temperature of maximum density (TMD). The system also displays diffusion anomalies [55], maxima of isothermal compressibility  $K_T$ , isobaric heat capacity  $C_P$  and the isobaric thermal expansion coefficient  $\alpha_P$  [48, 49, 56, 57, 58, 53] related to the anomalous behavior of water in the supercooled region.

##### 4.2. Dynamical slowing down of water in supercooled region.

The dynamical behavior of the model at low  $T$  has interesting features [52, 56, 57]. The dynamics of the HBs at constant  $P$  displays an increase of the correlation time when  $T$  is decreased. The increase is faster at higher  $T$  than at lower  $T$  and shows a crossover at the temperature when  $C_P$  has a maximum [56, 57]. Results clarify that the crossover is due to a structural change in the HBs network [56, 57]. The qualitative features of this crossover have been successfully compared to experimental results for confined water at increasing  $P$  [59]. In particular Franzese and de los Santos [52] have been showed that at high pressure ( $P \simeq 2000$  bar) the effect of HB is negligible due to the high enthalpic cost to form a HB and the correlation function decays as an exponential. At low  $P$  ( $P \simeq 1$  bar) the correlation is large also at long times and the system get stuck in a glassy state. The structural analysis shows that under these conditions the HB network develops gradually by decreasing  $T$  and traps the system in metastable configurations.

For intermediate value of pressure the correlation function  $C(t)$  is well described by a stretched exponential function

$$C(t) = C_0 e^{-\left(\frac{t}{\tau}\right)^\beta}, \quad (21)$$

where  $C_0$ ,  $\tau$  and  $\beta \leq 1$  are fitting constant ( $\beta = 1$  correspond to exponential decay). The quantity  $1 - \beta$  is a measure of the heterogeneity in the system. As we approach to a characteristic value of pressure  $P_{C'}$ ,  $\beta$  reaches its minimum value ( $\beta \simeq 0.4$ ). This is consistent with the experimental value of  $\beta \simeq 0.35$ , observed for intermediate scattering correlation function of water hydrating myoglobin at low hydration level ( $h = 0.35$  g H<sub>2</sub>O/g protein) [60, 61]. Therefore, Franzese and de los Santos result indicates that the system exhibits a largest amount of heterogeneity at  $P_{C'}$ . As we will discuss in the next section, this heterogeneity is the consequence of a large increase of cooperativity in the vicinity of  $P_{C'}$ .

#### 4.3. Thermodynamics of supercooled water.

Four scenarios have been proposed to explain the thermodynamics supercooled water. The *stability limit* scenario [62] hypothesizes that the limit of stability of superheated liquid water merges with the limit of stretched and supercooled water, giving rise to a single locus in the  $P - T$  plane, with positive slope at high  $T$  and negative slope at low  $T$ . The reentrant behavior of this locus would be consistent with the anomalies of water observed at higher  $T$ . As discussed by Debenedetti, thermodynamic inconsistency challenges this scenario [63].

The *liquid-liquid critical point* (LLCP) scenario [64] supposes a first order phase transition in the supercooled region between two metastable liquids at different densities: the low-density liquid (LDL) at low  $P$  and  $T$ , and the high-density (HDL) at high  $P$  and  $T$ . The phase transition line has a negative slope in the  $P - T$  plane and ends in a critical point. Numerical simulations for several models are consistent with this scenario [64, 65, 66, 67].

The *singularity-free* scenario [39] focuses on the anticorrelation between entropy and volume as cause of the large increase of response functions at low  $T$  and hypothesizes no HB cooperativity. The scenario predicts lines of maxima in the  $P - T$  for the response functions, similar to those observed in the LLCP scenario, but shows no singularity for  $T > 0$ .

The *critical-point-free* scenario [68] hypothesizes an order-disorder transition, with a possible weak discontinuity of density, that extends to  $P < 0$  and reaches the supercooled limit of stability of liquid water. This scenario would effectively predicts no critical point and a behavior for the limit of stability of liquid water as in the stability limit scenario.

As showed by Stokely et al. [54], all these scenarios may be mapped into the space of parameter  $J$  and  $J_\sigma$ , of the model presented in the previous section, i.e. the coupling constants of the covalent component of the HBs and the coupling constant of the many-body component of the HB interaction, respectively. In particular, Stokely et al. showed by mean field calculations and numerical simulations that the absence of the

many-body component leads to singularity free scenario, while a large value of the many-body component with respect to the covalent component give rise to the critical-point free/stability limit scenario [54].

By using estimate of these parameters from experimental results, the authors predict a liquid-liquid phase transition at low temperature and high pressure ending in a second critical point  $C'$  for water [54]. Therefore, following this prediction, the increasing fluctuations related to  $C_P$ ,  $K_T$  and  $\alpha_P$  of water under cooling are consequence of the liquid-liquid critical point  $C'$  in the supercooled region of water. By approaching  $C'$ , the correlation length  $\xi$  of the HBs increases. In particular for any  $P < P_{C'}$ , the critical pressure, there is a temperature  $T_W$  where the correlation length  $\xi(P)$  is maximum. The locus  $T_W(P)$ , called Widom line, converges toward  $C'$  with a negative slope in the  $P - T$  plane [49, 69]. By increasing  $P$  along the Widom line,  $\xi$  increases and diverges at  $P = P_{C'}$ . Therefore, the regions of cooperativity of HBs increase in size, leading to long cooperativity and, as a consequence, to larger heterogeneity in the dynamics as observed by Franzese and de los Santos [52] (discussed in the previous section).

Before discussing in more details the features of these cooperative regions, is worth mentioning that recent theoretical and experimental results on water hydrating lysozyme proteins at very low hydration level ( $h = 0.3$  g H<sub>2</sub>O/g protein) allow to explain the very low- $T$  phase diagram of water monolayer, at  $T \simeq 150$  K at ambient pressure [70]. This investigation reveals that at low  $P$  two structural changes take place in the HB network of the hydration shell. One at about 250 K is due to the building up of the HB network [57], and another at about 180 K is consequence of the cooperative reorganization of the HBs. These two structural changes give rise to two dynamical crossovers in the HB correlation time and the corresponding experimental quantity, the proton relaxation time [70]. By increasing  $P$ , approaching  $P_{C'}$ , the two structural changes merge and at  $P_{C'}$  lead to diverging fluctuations associated to the liquid-liquid critical point, as discussed in a recent work by Mazza et al. [71].

## 5. Geometrical description of clusters of correlated HBs

As discussed in the previous section, a water monolayer between hydrophobic plates separated by less than 1 nm, has a complex phase behavior at low  $T$  below the limit of stability of bulk liquid water. The same phase diagram compares well with experiments with water monolayer hydrating a complex substrate formed by proteins at low hydration level [60, 61]. This can be understood if we admit that the main effect of the protein substrate at low hydration is to induce in the first layers of hydrating water a structure that is inconsistent with any possible crystal. Therefore, the substrate inhibits the crystallization, but does not inhibit the water-water HB formation. It is, therefore, interesting to understand how the region of correlated HB builds up and give rise to the cooperative rearrangement and the liquid-liquid phase transition.

To this goal we follow an approach that has been validated during the last three decades to describe critical phase transitions. It consists in a percolation approach

elaborated in 1980 by Coniglio and Klein [72] for ferromagnetic systems and related to a mathematical mapping introduced by Fortuin and Kasteleyn [73] and to Swendsen-Wang [74] and Wolff [75] techniques for cluster MC methods. The Coniglio-Klein approach, called *random-site-correlated-bond percolation*, was extended ferromagnetic systems with many states [76] and spin-glass-like systems [77, 78, 79, 80]. In particular, in Ref. [72] it was proved that the clusters defined following the rules of this specific type of percolation statistically coincide with the region of thermodynamically correlated variables. Moreover, in Ref. [78] it was proved that this result holds as long as the system has no frustration due to competing interactions. Since in the case considered here there are no competing interactions, we can follow the percolation approach to define clusters of water molecules with statistically correlated HBs.

As described in Ref. [43], we adopt the Wolff cluster MC algorithm [53] to study the cooperative regions and their length scale. Thanks to the fact that a cluster represents a region of water molecules with statistically correlated HBs, the algorithm allows to equilibrate the system at any  $T$  [53].

By definition, two variables  $\sigma_{ij}$  and  $\sigma_{ji}$  belong to the same cluster with probability

$$p = \min\{\delta_{\sigma_{ij}\sigma_{ji}}, 1 - \exp[-(J - Pv_{\text{HB}})/kT]\} \quad (22)$$

if they belong to nearest neighbor molecules, or with probability

$$p_{\sigma} = \min\{\delta_{\sigma_{il}\sigma_{ik}}, 1 - \exp(-J_{\sigma}/kT)\} \quad (23)$$

if they belong to the same water molecule  $i$ .

The size of a cluster is given by the total number of  $\sigma_{ij}$  variables belonging to the cluster. For each four  $\sigma_{ij}$  in a cluster we have, on average, one water molecule in the cluster. The average linear size of finite (non percolating) cluster is, for the mapping discussed above, statistically equivalent to the correlation length of the HBs. Moreover, it is possible to prove [76] that each thermodynamic quantity, such as the compressibility, can be described in terms of an appropriate moment of the finite cluster distribution.

By approaching the critical point  $C'$ , we observe that the largest cluster percolates and its linear size becomes comparable to the system size. Under these conditions, the correlation length  $\xi$  diverges. While away from  $C'$  the distribution  $n(s)$  of cluster of linear size  $s$  decays as an exponential,  $n(s)$  has a power law decay near  $C'$  (Fig. 2) consistent with the theory [78].

From general considerations it is possible to show that  $n(s) \sim s^{-\tau}$ , where the exponent  $\tau$  is related to the fractal dimension  $D_F$  of the system  $\tau = 1 + d/D_F$ , and  $d = 2$  is the embedding (euclidean) dimension. A preliminary estimate  $\tau \simeq 2$  suggests that the clusters of correlated HBs are compact with  $D_F \sim 2$  [81]. Therefore, the mapping of the thermodynamic systems into a percolation problem allows us to give a geometrical description of the correlated HBs.

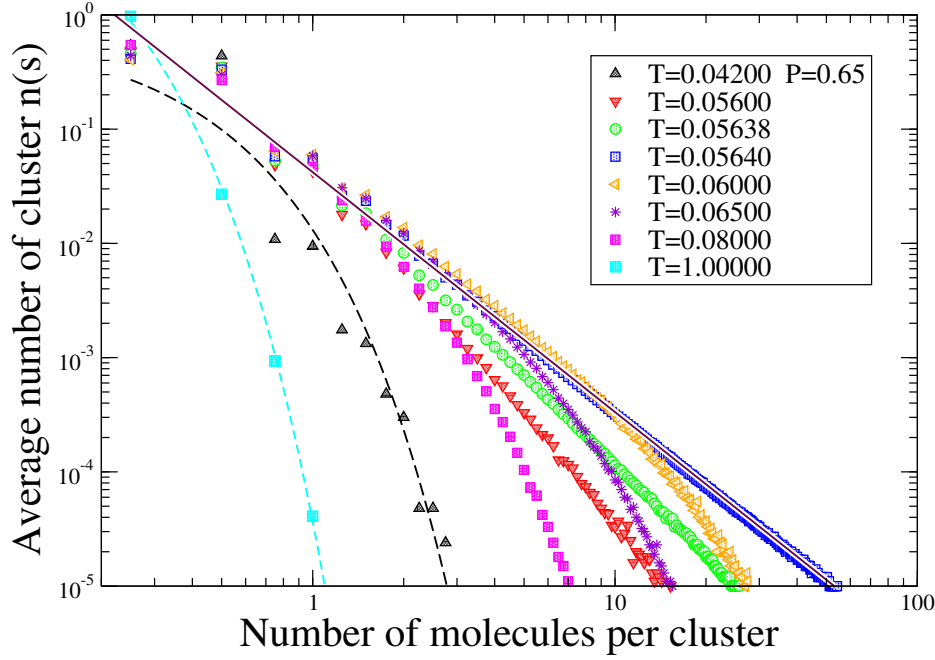


**Figure 2.** Distribution  $n(s)$  of clusters with finite size  $s$  formed by correlated hydrogen bonds (HBs) in a non-crystallizing water monolayer. Calculations are for  $P = 1.93 \text{ GPa} \simeq P_{C'}$ , the liquid-liquid critical pressure, and different values of temperature for system with  $N = 4 \times 10^4$  water molecules. For  $T = 173.84 \text{ K} \simeq T_{C'}$ , the liquid-liquid critical temperature, calculations (blue square points) decays as a power law  $n(s) \sim s^{-\tau}$  with  $\tau = 2.1 \pm 0.1$ , as expected from theory near a critical point [78]. Consistent with the theory, we find that  $n(s)$  cannot be described by a power law decay away from the critical point. This is the case, for example, at  $T = 173.83 \text{ K}$  (green circles) and  $T = 176.35 \text{ K}$  (orange triangles). We find that at temperature far from the critical temperature,  $n(s)$  has an exponential decay, as expected. This is the case, for example, at  $T = 833.08 \text{ K}$  (light blue square) and  $T = 163.80 \text{ K}$  (black triangles). Continuous line is the power law fit, while dashed line are exponential fits.

## 6. Free energy landscape analysis

The percolation approach allows us to adopt a cluster MC dynamics that is very efficient at low  $T$  [53]. Therefore, we can equilibrate the system at low  $P$  around the  $T_W(P)$ , the temperature of maximum correlation length  $\xi$ , and around the temperature  $T_{LL}$  of liquid-liquid coexistence at high  $P$ , and calculate the free energy landscape for the system.

By definition, the Gibbs free energy is

$$G/k_B T \equiv -\ln \mathcal{P}(H, \rho), \quad (24)$$

where  $\mathcal{P}(H, \rho)$  is the density of states with enthalpy  $H \in [H, H + \delta H]$  and density  $\rho \in [\rho, \rho + \delta \rho]$ , with  $\delta H$  and  $\delta \rho$  infinitesimal increments. In Fig. 3 we show  $G$  as a function of energy per particle  $E/N$  and the density  $\rho$  with two equivalent minima straddling the line of phase transition. The two minima, equivalent within the numerical precision, correspond to two coexisting phases with different density and energy. The one at higher

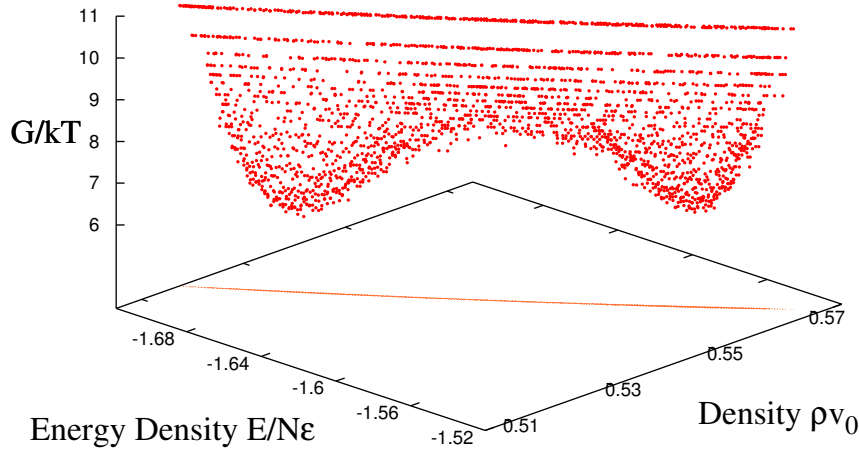


**Figure 3.** Gibbs free energy for a water monolayer with  $N = 4 \times 10^4$  water molecules at  $P = 1.98$  GPa and  $T = 158$  K. The two minima, one at low energy and density, and the other at high energy and density, represent respectively the LDL phase and HDL phase of the system. The projection of  $G$  on the plane  $E/N - \rho$  shows that there is a linear relation between the accessible energies and density for the coexisting states. The same value of the minima marks the coexistence of the two phases.

density and energy represents the HDL phase. The other at lower density and energy represents the LDL phase. Approaching  $C'$  the two minima get closer and the density separation disappears, as expected at the critical point. These results are consistent with the mean field free energy analysis of Ref. [53, 82], where the Gibbs free energy is calculated as function of the HB order parameters relevant at the structural transition at high  $P$  and low  $T$ . In the mean field analysis the minima of  $G$  are separated at high  $P$ , but merge for  $P$  approaching  $P_{C'}$ . All these results are consistent with the behavior of  $C_P$ ,  $K_T$  and  $\alpha_P$  whose maxima move to lower  $T$  as  $P$  is increased [56, 48, 56, 58]. The loci of the maxima of  $C_P$ ,  $K_T$  and  $\alpha_P$  merge in the vicinity of  $C'$  and the amplitude of their maxima increases approaching  $C'$ .

## 7. A model for protein in water

In the previous section we define a coarse-grained model for a water monolayer and we show that the model compares well with experiments for protein shell–water and that it predicts a complex phase diagram for low  $T$ , below the limit of stability of bulk liquid water, and high  $P$ . As discussed in the introduction, under these conditions folded proteins are destabilized. Following our discussion about how could be relevant to take into account the HB free energy to explain the lost of stability of folded proteins, It is

intriguing to test if the proposed water model could give insight into the mechanism of unfolding.

To this goal we modify the water model to introduce the effect of the protein-water interface. For sake of the simplicity, we will limit our discussion to the case of a single protein embedded into a water monolayer. Although far from the complex studies of a protein embedded into bulk water, the model gives instructive results.

The simplest protein that we can consider is a hydrophobic homopolymer, schematized as a self avoiding chain (Fig. (4)). Following the discussion by Muller [15], we require that, consistent with experiment, water molecules in contact with a hydrophobic monomer have larger decrease of enthalpy upon HB formation. Also consistent with Muller-Lee-Graziano discussion [25], the fraction of broken HBs at the hydrophobic interface is larger than the fraction of broken HBs in the bulk.

The first requirement is achieved by adding a term to the water Hamiltonian Eq. (18)

$$\mathcal{H}_s = -\lambda J \sum_{\langle ij \rangle_s} n_i n_j \delta_{\sigma_{ij}} \delta_{\sigma_{ji}}, \quad (25)$$

where the sum is taken over nearest neighbor water molecules in the protein hydration shell (Fig. 4), and  $\lambda > 0$  is an adjustable parameter accounting for the larger enthalpy decrease for HBs in the hydration shell. Hence, for HB formed between water molecules in the shell, the enthalpy variation is  $-J(1 + \lambda) + P v_{\text{HB}}$ , and the total enthalpy for protein into water is

$$H_{\text{tot}} = H + \mathcal{H}_s, \quad (26)$$

where  $H$  is given by Eq. (18).

The second requirement of Muller-Lee-Graziano approach, i.e. a larger number of broken HBs at the interface, is achieved by volume exclusion. Once a cell of our system is occupied by a protein monomer, it cannot be occupied by a water molecule. Therefore, a water molecule, in the hydration shell cannot form the HB in the direction of the monomer and loses at least one HB (it can lose more if it has more monomers as nearest neighbors, as shown in Fig. 4).

In the following section we will define the algorithm adopted to generate protein equilibrium configurations. To this propose we follow a MC procedure that mimics the dynamics at large time scales.

### 7.1. Monte Carlo algorithm

We perform MC simulations in the  $NPT$  ensemble. In every MC step we choose a cell at random. If it is occupied by a water molecule, we change randomly one of its  $\sigma$  variables. If it is occupied by a monomer and if the monomer is in a corner configuration (Fig. 5A) then we swap its position with the position of the water molecules in the cell in the opposite corner. By doing this, we keep the inter-monomer distances constant.

If the cell, picked at random, is occupied by a monomer not in a corner configuration, no displacement is performed because it would change the inter-monomer



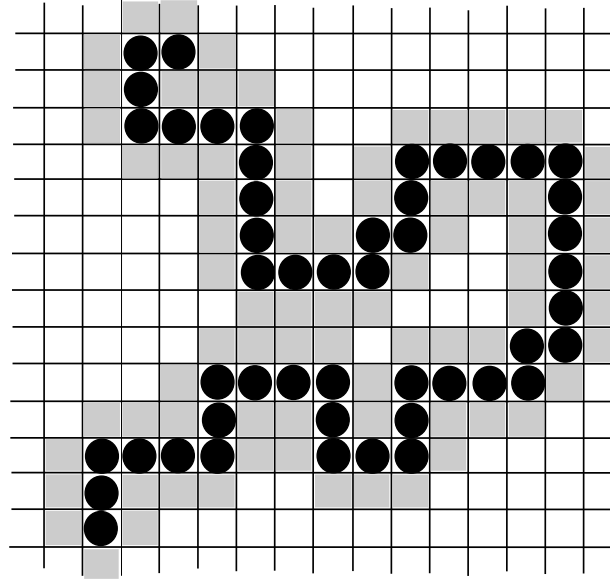


**Figure 4.** Example of configuration of a homopolymer in the coarse-grained model. Each cell is occupied either by a water molecule (white and gray cells) or a hydrophobic homopolymer monomer (cells with a full black circle). The gray cells represents the sites occupied by shell water. The enthalpy gain for HB formation between shell water molecules is larger than that between bulk water molecules, according to the Eq. 25. Shell water molecules cannot form hydrogen bonds with nearest neighbors hydrophobic monomers.

distance. This limitation is introduced in order to avoid in the free energy any term accounting for the elastic energy of the homopolymer. The effects of this elastic contribution are for the moment outside of the scope of the present work.

Finally, as in the cases discussed in the previous section, to keep the pressure of the system constant, every  $N$  random changes of the cell variables (where  $N$  is the total number of cells in the system), we attempt to rescale all the system volume by a factor that is tuned in a way to guaranty 50% of acceptance ratio. All the MC moves described above are accepted or rejected according to the Boltzmann factor associated to the enthalpy change caused by the move.

In order to study the folding-unfolding process of the proteins we calculate the number of contact points  $N_{\text{cpts}}$  as illustrated in Fig. (5). In this calculation we do not count the monomers that are adjacent along the homopolymer.

## 8. Preliminary results for hydrated homopolymers

We study a system with  $N$  water molecules and a hydrophobic homopolymer chain with  $N_m$  monomers. In our preliminary simulations we used  $N = 650$  or  $N = 1000$  and  $N_m = 12$  or  $N_m = 50$ . The parameters are chosen, for consistency, as in previous analysis [83]:  $\epsilon = 5.8$  kJ/mol,  $J = 2.9$  kJ/mol,  $J_\sigma = 0.29$  kJ/mol,  $v_0 = hr_0^2$ ,  $h = 7$  Å,  $v_{\text{HB}}/v_0 = 0.5$  and  $q = 6$ . We choose  $\lambda = 0.7$  for the larger decrease of enthalpy at the

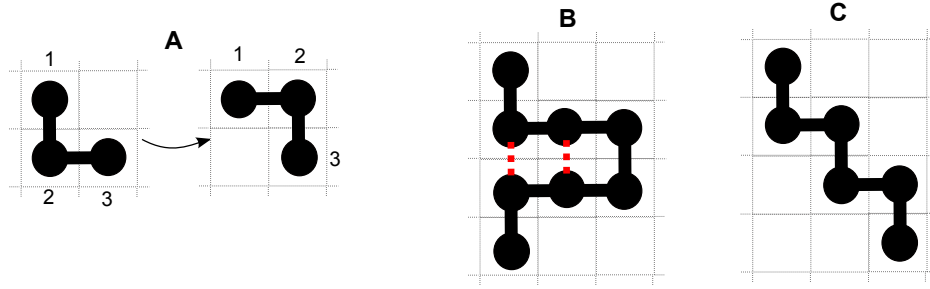


**Figure 5.** A) Monomer 2 is in a corner configuration and can be displaced from the configuration on the left to the configuration on the right and *vice versa*. B) Homopolymer configuration with two contact points, indicated with dotted lines. C) Homopolymer configuration without contact points.

hydrophobic interface.

Our results display a non monotonic behavior of  $N_{\text{cpts}}$  as function of  $T$  at low  $P$ . At high pressure we observe an region in the  $P - T$  plane where the number of contact points is at least 51% of the maximum possible number. By definition, we consider these configurations as belonging to the set of folded states. We observe that the region of folded states is included within a larger region in the  $P - T$  plane where the number of contact points is at least 49% of the maximum possible number. By definition, we consider those configurations as members of the set of state representing the molten globule [84].

We find that the region of folded states has an elliptic shape that resembles the theoretical prediction (Fig. 1). In particular, we observe that a folded protein unfolds upon cooling, giving rise to the cold denaturation process. It also unfold by increasing the pressure as expected by pressure denaturation (Fig. 6). Since our stability region is at high  $P$ , we are also able to observe the unfolding by decreasing the pressure, a phenomena that is predicted by general theoretical considerations, as discussed in the introduction. We also find that the axes of the elliptical stability region are tilted as expected (Fig. 1).

## 9. Conclusions

The behavior of supercooled water is still under debate and the presence of a second critical point  $C'$  could be relevant to understand how the structure of liquid water changes around proteins and how affects protein properties. Experiments of water confined in nano-structures offer the possibility to access a range of temperatures where bulk liquid water would not be stable and would form ice. Hence, confinement allows to study water under conditions that are relevant in biological systems.

Despite the growing interest of the scientific community in water at hydrophobic and hydrophilic interfaces, it is still unclear how the interaction with the confining surfaces affects the thermodynamics of water. For example, recently Strekalova et al. [83] observed that the fluctuations of supercooled water confined into a hydrophobic

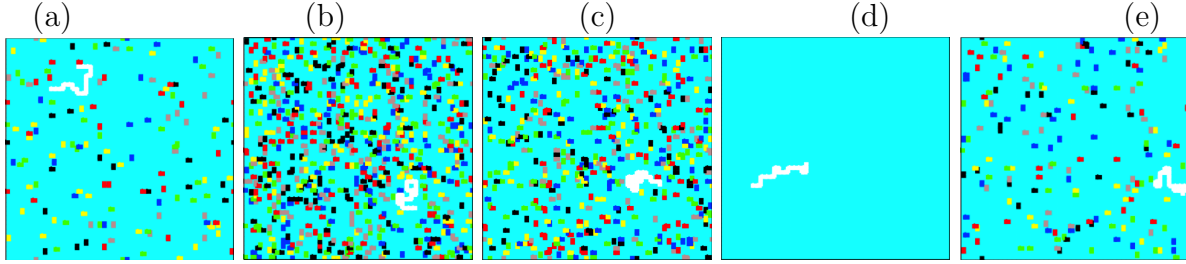


**Figure 6.** Typical configurations of folding-unfolding of a coarse-grained protein suspended in water at different temperatures  $T$  and high pressures  $P$ . The protein is represented as a fully hydrophobic chain (in white), surrounded by water molecules (turquoise background). We use different color for water to indicate the different orientations of the HBs. (a) At high  $P$  and high  $T$ , the protein unfolds and the number of HBs (colored sticks) of surrounding water is small. (b) At the same pressure but lower  $T$ , the protein collapses in a molten globule state. (c) At lower  $T$  the protein folds, while the surrounded water has a large number of HBs. (d) At much lower  $T$  we observe cold denaturation of the protein when the number of HBs is largely reduced (zero in the configuration represented here). (e) At higher  $P$  the denaturation occurs at higher  $T$ , and the mechanism of unfolding seems to be dominated by the reduction of HBs also under these conditions.

porous material are drastically smaller than those of bulk water. They found that the response functions  $C_P$ ,  $\alpha_P$  and  $K_T$  are largely reduced as a consequence of the interaction with the porous medium. An extreme consequence of this change is the disappearing of the liquid-liquid phase transition at high pressures [83]. Therefore, further work is necessary to clarify the many issues related to the dynamics and thermodynamics of water at the interfaces.

Here we presented a coarse-grained model for a monolayer of water and its extension to the case of solvated proteins. The model takes into account the cooperativity between HBs and has been studied by simulations and mean field calculations. Previous results about the phase diagram, the diffusivity properties, the response functions  $C_P$ ,  $\alpha_P$  and  $K_T$  of the model and the connection of these quantities with the HBs dynamics are in agreement with experimental results and validate the model.

We adopted this model in the context of protein folding. For the sake of simplicity we consider the case of a protein schematized as a self-avoiding hydrophobic homopolymer. Following Muller analysis [15], we assume that the network of HBs is perturbed by the presence of hydrophobic solute with large size.

Our preliminary results reproduce hot, cold and pressure denaturation as well as the existence of intermediate states (molten globule). We find that the stability region for folded protein has the theoretically expected elliptic shape in the  $P - T$  plane. Further work is in progress to elucidate the relevant mechanism ruling protein stability.

## Acknowledgments

We thank for enlightening discussion G. Caldarelli, P. de los Rios, P. G. Debenedetti, C. M. Dobson, M. Vendruscolo. G.F. thanks for collaboration and helpful discussions M. C. Barbosa, S. V. Buldyrev, F. Bruni, S.-H. Chen, A. Hernando-Martínez, P. Kumar, G. Malescio, F. Mallamace, M. I. Marqués, M. G. Mazza, A. B. de Oliveira, S. Pagnotta, F. de los Santos, H. E. Stanley, K. Stokely, E. G. Strekalova, P. Vilaseca, and the Spanish Ministerio de Ciencia e Innovación Grants FIS2009-10210 (co-financed FEDER) for support.

- [1] Ravindra R, Winter R, On the temperature-pressure free-energy landscape of proteins, *Chem Phys Chem* 2003;4:359-365.
- [2] Pastore A, Martin S R, Politou A, Kondapalli K C, Stemmeler T, Temussi P A, Unbiased Cold Denaturation: Low- and High-Temperature Unfolding of Yeast Frataxin under Physiological Conditions, *J Am Chem Soc* 2007;129:5374-5375.
- [3] Privalov P L, Cold Denaturation of Proteins, *Crit Rev Biochem Mol Biol* 1990;25:281-305.
- [4] Nash D, Jonas J, Structure of the pressure-assisted cold denatured state of ubiquitin, *Biochem Biophys Res Commun* 1997;238:289-291.
- [5] Nash D, Jonas J, Structure of the pressure-assisted cold denatured lysozyme and comparison with lysozyme folding intermediates, *Biochemistry* 1997;36:14375-17383.
- [6] Meersman F, Smeller L, Heremans K, Pressure-assisted cold unfolding of proteins and its effects on the conformational stability compared to pressure and heat unfolding, *High Press Res* 2000;19:263-268.
- [7] Goossens K, Smeller L, Frank J, Heremans K, Pressure tuning spectroscopy of bovin pancreatic trypsin inhibitor: a high pressure FT-IR study, *Eur J Biochem* 1996;236:254-262.
- [8] Meersman F, Dobson C M, Heremans K, Protein unfolding, amyloid fibril formation and configurational energy landscapes under high pressure conditions, *Chem Soc Rev* 2006;35:908-917.
- [9] Hummer G, Garde S, Garcia A E, Paulaitis M E, The pressure dependence of hydrophobic interaction is consistent with the observed pressure denaturation of proteins, *Proc Natl Acad Sci USA* 1998;95:1552-1555.
- [10] Kunugi S, Yamamoto H, Makino M, Tada T, Uehara-Kunugi Y, Pressure-assisted cold-denaturation of carboxipeptidase Y, *Bull Chem Soc Jpn* 1999;72:2803-2806.
- [11] Hawley S A, Reversible pressure-temperature denaturation of chymotrypsinogen, *Biochemistry* 1971;10:2436-2442.
- [12] Smeller L, Pressure-temperature phase diagrams of biomolecules, *Biochim Biophys Acta* 2002;1595:11-29.
- [13] Lau K F, Dill K A, A lattice statistical mechanics model of the conformational and sequence spaces of proteins, *Macromolecules* 1989;22:3986-3997.
- [14] Frank H S, Evans M W, Free Volume and Entropy in Condensed Systems III. Entropy in Binary Liquid Mixtures; Partial Molal Entropy in Dilute Solutions; Structure and Thermodynamics in Aqueous Electrolytes, *J Chem Phys* 1945;13:507-533.
- [15] Muller N, Search for a realistic view of hydrophobic effects, *Acc Chem Res* 1990;23:23-28.
- [16] Mirejovsky D, Arnett E M, Heat capacity of the solution for alcohols in polar solvents and the new view of hydrophobic effects, *J Am Chem Soc* 1983;105:1112-1117.
- [17] Geiger A, Rahman A, Stillinger F H, Molecular Dynamics Study of the Hydration of Lennard-Jones Solutes, *J Chem Phys* 1979;70:263-276.
- [18] van Belle D, Wodak S J, Molecular dynamics study of methane hydration and methane association in a polarizable water phase, *J Am Chem Soc* 1993;115:647-652.

- [19] Lee B, In An anatomy of hydrophobicity; Eds: Eisenfeld J, DiLisi C; Elsevier, North-Holland: Amsterdam, 1985.
- [20] Lee B, Solvent reorganization contribution to the transfer thermodynamics of small nonpolar molecule, *Biopolymers* 1991;31:993-1008.
- [21] Madan B, Lee B, Role of hydrogen bonds in hydrophobicity: the free energy of cavity formation in water models with and without the hydrogen bonds, *Biophys Chem* 1994;51:279-289.
- [22] Finney J L, Soper A K, Solvent structure and perturbations in solutions of chemical and biological importance, *Chem Soc Revs* 1994;1:1-10.
- [23] Ben-Naim A, Hydrophobic interaction and structural changes in the solvent, *Biopolymers* 1975;14:1337-1355.
- [24] Souza L E S d, Ben-Amotz D J, Hard Fluid Model for Molecular Solvation Free Energies, *J Chem Phys* 1994;101:9858-9863.
- [25] Lee B, Graziano G, A Two-State Model of Hydrophobic Hydration That Produces Compensating Enthalpy and Entropy Changes, *J Am Chem Soc* 1996;22:5163-5168.
- [26] Rios P D L, Caldarelli G, Putting proteins back into water, *Phys Rev E* 2000;62:8449-8452.
- [27] Caldarelli G, Rios P D L, Cold and Warm Denaturation of Proteins, *J Biol Phys* 2001;27:229-241.
- [28] Rios P D L, Caldarelli G, Cold and Warm Denaturation of Hydrophobic Polymers, *cond-mat/9903394v3* 2008.
- [29] Salvi G, Rios P D L, Vendruscolo M, Effective Interactions Between Chaotropic Agents and Proteins, *Proteins: Structure, Function, Bioinformatics* 2005;261:492499.
- [30] Bruscolini P, Casetti L, Lattice model for cold and warm swelling of polymers in water, *Phys Rev E* 2000;61:2208-2211.
- [31] Bruscolini P, Casetti L, Bethe approximation for a model of polymer solvation, *Phys Rev E* 2001;64:051805.
- [32] Makhatadze G I, Privalov P L, Energetics of protein structure, *Adv Protein Chem* 1995;47:307-425.
- [33] Silverstain K A T, Haymet A D J, Dill K A, A Simple Model of Water and the Hydrophobic Effect, *J Am Chem Soc* 1998;120:3166-3175.
- [34] Dias C L, Ala-Nissila T, Karttunen M, Vattulainen I, Grant M, Microscopic mechanism for cold denaturation, *Phys Rev Lett* 2008;100:118101.
- [35] Ben-Naim A J, Statistical Mechanical Study of Hydrophobic Interaction. I. Interaction between Two Identical Nonpolar Solute Particles, *Chem Phys* 1971;54:1387 .
- [36] Yoshidome T, Harano Y, Kinoshita M, Hydrophobicity at low temperatures and cold denaturation of a protein, *Phys Rev E* 2009;79:011912.
- [37] Kusalik P G, Patey G N, The solution of the reference hypernetted-chain approximation for water-like models, *Mol Phys* 1988;65:1105-1119.
- [38] Marqus M I, Borreguero J M, Stanley H E, Dokholyan N V, Possible Mechanism for Cold Denaturation of Proteins at High Pressure, *Phys Rev Lett* 2003;91:138103.
- [39] Sastry S, Debenedetti P G, Sciortino F, Stanley H E, Singularity-free interpretation of the thermodynamics of supercooled water, *Phys Rev E* 1996;53:6144-6154.
- [40] Zhang J, Peng X, Jonas A, Jonas J, NMR study of the cold, heat, and pressure unfolding of ribonuclease A, *Biochemistry* 1995;34:8631-8641.
- [41] Lassalle M W, Yamada H, Akasaka K, The pressure-temperature free energy-landscape of staphylococcal nuclease monitored by  $^1\text{H}$  NMR, *J Mol Biol* 2000;298:293-302.
- [42] Patel B A, Debenedetti P G, Stillinger F H, Rossky P J, A water-explicit lattice model of heat-, cold-, and pressure-induced protein unfolding, *Biophys J* 2007;93:4116-4127.
- [43] Franzese G, Bianco V, Iskrov S, Water at the interface with proteins, *Food Biophys* 2010; arXiv:1010.4984v1, in print.
- [44] Soper A, Ricci M, Structures of high-density and low-density water, *Phys Rev Lett* 2000;84:2881-2884.
- [45] Kumar P, Buldyrev S V, Starr F W, Giovanbattista N, Stanley H E, Thermodynamics, structure, and dynamics of water confined between hydrophobic plates, *Phys Rev E* 2005;72:051503.

- [46] Franzese G, Stanley H E, A theory for discriminating the mechanism responsible for the water density anomaly, *Physica A* 2002;314:508-513.
- [47] Franzese G, Stanley H E, Liquid-liquid critical point in a Hamiltonian model for water: analytic solution, *J Phys Condens Matter* 2002;14:2201-2209.
- [48] Franzese G, Marqués M I, Stanley H E, Intramolecular coupling as a mechanism for a liquid-liquid phase transition, *Phys Rev E* 2003;67:011103.
- [49] Franzese G, Stanley H E, The Widom line of supercooled water, *J Phys Condens Matter* 2007;19:205126.
- [50] Debenedetti P G, *Metastable Liquids: Concepts and Principles*, Princeton University Press, Princeton, 1996.
- [51] Ricci M A, Bruni F, Giuliani A, Similarities between confined and supercooled water, *Faraday Discuss* 2009;141:347-358.
- [52] Franzese G, Santos F d l, Dynamically Slow Processes in Supercooled Water Confined Between Hydrophobic Plates, *J Phys Condens Matter* 2009;21:504107.
- [53] Mazza M G, Stokely K, Strekalova E G, Stanley H E, Franzese G, Cluster Monte Carlo and numerical mean field analysis for the water liquid-liquid phase transition, *Comp Phys Comm* 2009;180:497-592.
- [54] Stokely K, Mazza M G, Stanley H E, Franzese G, Effect of hydrogen bond cooperativity on the behavior of water, *Proc Natl Acc Sci USA* 2010;107:1301-1306.
- [55] Santos F d l, Franzese G in preparation.
- [56] Kumar P, Franzese G, Stanley H E, Dynamics and thermodynamics of water, *J Phys Condens Matter* 2008;20:244114.
- [57] Kumar P, Franzese G, Stanley H E, Predictions of Dynamic Behavior under Pressure for Two Scenarios to Explain Water Anomalies, *Phys Rev Lett* 2008;100:105701.
- [58] Franzese G, Martínez A H, Kumar P, Mazza M G, Stokely K, Strekalova E G, Santos F d l, Stanley H E, Phase transitions and dynamics of bulk and interfacial water, *J Phys Condens Matter* 2010;22:284103.
- [59] Chu X -q, Faraone A, Kim C, Fratini E, Baglioni P, Leao J B, Chen S -H, Proteins Remain Soft at Lower Temperatures under Pressure, *J Phys Chem B* 2009;113:5001-5006.
- [60] Settles M, Doster W, Anomalous diffusion of adsorbed water: A neutron scattering study of hydrated myoglobin, *Faraday Discuss* 1996;103:269-279.
- [61] Doster W, The protein-solvent glass transition, *Biochimica et Biophysica Acta* 2010;1804:3-14.
- [62] Speedy R J, Limiting forms of the thermodynamic divergences at the conjectured stability limits in superheated and supercooled water, *J Phys Chem* 1982;86:3002-3005.
- [63] Debenedetti P G, Supercooled and glassy water, *J Phys Condens Matter* 2003;15:R1669R1726.
- [64] Poole P, Sciortino F, Essmann U, Stanley H E, Phase-Behavior Of Metastable Water, *Nature* 1992;360:324-328.
- [65] Poole P H, Sciortino F, Grande T, Stanley H E, Angell C A, Effect of Hydrogen Bonds on the Thermodynamic Behavior of Liquid Water, *Phys Rev Lett* 1994;73:16321635.
- [66] Tanaka H, A self-consistent phase diagram for supercooled water, *Nature* 1996;380:328330.
- [67] Tanaka H, Phase behaviors of supercooled water: Reconciling a critical point of amorphous ices with spinodal instability, *J Chem Phys* 1996;105:50995111.
- [68] Angell C A, Insights into Phases of Liquid Water from Study of Its Unusual Glass-Forming Properties, *Science* 2008;319:582-587.
- [69] Xu L, Kumar P, Buldyrev S V, Chen S -H, Poole P H, Sciortino F, Stanley H E, Relation between the Widom line and the dynamic crossover in systems with a liquid-liquid phase transition, *Proc Natl Acad Sci USA* 2005;102:16558-16562.
- [70] Mazza M G, Stokely K, Pagnotta S E, Bruni F, Stanley H E, Franzese G, Two dynamic crossovers in protein hydration water and their thermodynamic interpretation, *arXiv:0907.1810v1*, 2009.
- [71] Mazza M G, Stokely K, Stanley H E, Franzese G, Anomalous specific heat of supercooled water, *arXiv:0807.4267*, 2008.

- [72] Coniglio A, Klein W, Cluster and Ising critical droplets: a renormalization group approach, *J Phys A* 1980;12:2775-2780.
- [73] Fortuin C M, Kasteleyn P W, On the random cluster model. I. Introduction and relation to other models, *Physica (Amsterdam)* 1972;57:536-564.
- [74] Swendsen R H, Wang J S, Nonuniversal critical dynamics in Monte Carlo simulations, *Phys Rev Lett* 1987;58:86-88.
- [75] Wolff U, Collective Monte Carlo Updating for Spin Systems, *Phys Rev Lett* 1989;62:361-364.
- [76] Coniglio A, Liberto F d, Monroy G, Peruggi F, Exact relations between droplets and thermal fluctuations in external field, *J Phys A* 1989;22:L837-L842.
- [77] Cataudella V, Franzese G, Nicodemi M, Scala A, Coniglio A, Critical clusters and efficient dynamics for frustrated spin models, *Phys Rev Lett* 1994;72:1541-1544.
- [78] Franzese G, Cluster analysis for percolation on a two-dimensional fully frustrated system, *J Phys A* 1996;29:7367-7375.
- [79] Franzese G, Potts fully frustrated model: Thermodynamics, percolation, and dynamics in two dimensions, *Phys Rev E* 2000;61:6383-6391.
- [80] Franzese G, Cataudella V, Coniglio A, Invaded cluster dynamics for frustrated models, *Phys Rev E* 1998;57:8893.
- [81] Bianco V, Franzese G, in preparation.
- [82] Franzese G, Stokely K, Chu X -q, Kumar P, Mazza M G, Chen S -H, Stanley H E, Pressure effects in supercooled water: comparison between a 2D model of water and experiments for surface water on a protein, *J Phys Condens Matter* 2008;20:494210.
- [83] Strekalova E G, Mazza M G, Stanley H E, Franzese G, Large decrease of fluctuations for supercooled water in hydrophobic nanoconfinement, *arXiv:1010.0693v1*, 2010.
- [84] We thanks M. Vendruscolo for discussing this point.
- [85] Stillinger F H, Structure in aqueous solutions of nonpolar solutes from the standpoint of scaled-particle theory, *J Sol Chem* 1973;2:141-158.
- [86] Franzese G, Coniglio A, Phase transitions in the Potts spin-glass model, *Phys Rev E* 1998;58:2753-2759.
- [87] tenWolde P R, Frenkel D, Enhancement of protein crystal nucleation by critical density fluctuations, *Science* 1997;277:1975-1978.
- [88] Franzese G, Malescio G, Skibinsky A, Buldyrev S V, Stanley H E, Metastable liquid-liquid phase transition in a single-component system with only one crystal phase and no density anomaly, *Phys Rev E* 2002;66:051206.
- [89] Stokely K, Mazza M, Stanley H E, Franzese G, Metastable Systems under Pressure, Eds: Rzoska S J, Drozd-Rzoska A, Mazur V A; Springer; pp 197-216, 2010.